Copy No. _____

Defence Research and Development Canada
Recherche et développement pour la défense Canada

DEFENCE R&D DÉFENSE

Sea Surface Infrared Radiance Simulator

Part 2: Sky radiance and trailing wake integration

Vivian Issa
Zahir A. Daya

Defence R&D Canada – Atlantic

Technical Memorandum
DRDC Atlantic TM 2011-325
August 2012

Canada

This page intentionally left blank.

Sea Surface Infrared Radiance Simulator

Part 2: Sky radiance and trailing wake integration

Vivian Issa
Zahir A. Daya

Defence Research and Development Canada – Atlantic
Technical Memorandum
DRDC Atlantic TM 2011-325
August 2012

Abstract

In a previous paper, we developed a sea surface radiance simulator (SSRS) for modeling and simulating the sea surface radiance of the ambient sea surface in the infrared. In this report, we present two additional models in our simulator. A sky radiance model based on third party software ShipIR and atmospheric propagation software MODTRAN are incorporated to include a realistic distribution of sky radiance. A model of the turbulent wake roughness and temperature spatial variation are presented and a model of the turbulent wake radiance is implemented in our simulator. Our results show that the sea surface radiance is highly affected by the receiver position. In the turbulent wake, decreasing the receiver zenith angle decreases the reflected sky radiance on the sea surface and increasing the receiver zenith angle will decrease the thermal emitted sea surface radiance. This strong dependence results in positive or negative wake contrast radiances at different receiver angles.

Résumé

Lors d'une publication antérieure, nous avons développé un simulateur de la radiance infrarouge de la surface de l'eau (SSRS). Dans ce document, nous présentons deux modules ajoutés à notre simulateur. Un modèle de la radiance du ciel basé sur le logiciel ShipIR qui utilise le logiciel MODRAN de la propagation atmosphérique a été incorporé dans notre simulateur afin d'inclure une distribution réaliste de la radiance du ciel. De plus, nous avons implémenté un modèle du sillage turbulent avec une dépendance spatiale de la rugosité et de la température de la surface de l'eau. Nos résultats montrent que la radiance de la surface de l'eau est grandement affectée par la position du récepteur. La diminution de l'angle zénith du récepteur diminue la radiance réfléchie sur la surface de l'eau tandis que son augmentation diminue la radiance émise de la surface de l'eau. Cette dépendance crée un contraste positif ou négatif entre la radiance du sillage et celle de la surface de l'eau ambiante tout dépendamment de la position du récepteur.

This page intentionally left blank.

Executive summary

Sea Surface Infrared Radiance Simulator: Part 2: Sky radiance and trailing wake integration

Vivian Issa, Zahir A. Daya; DRDC Atlantic TM 2011-325; Defence Research and Development Canada – Atlantic; August 2012.

Background: Ship propellers leave behind them long scars, called trailing wakes, which can be observed up to many kilometers and for several minutes. Observed in detail, the trailing wake is composed of three features: the Kelvin wake, the turbulent wake, and the white water wake. The turbulent wake is a subject of interest in several types of surveillance such as optical, SAR, Radar, Microwave as well as infrared. In the infrared, these features are even richer in information as not only the orientation of the sea surface facet and the ambient radiance affect the sea surface radiance but so does the sea surface itself which acts as a thermal source. As the sea temperature often varies significantly with depth, the turbulent sea-water created by the mixing effect of the propulsion system has a different temperature than the ambient sea surface and hence a different infrared radiance.

Principal results: In a previous paper, we developed a simulator for modeling and simulating the sea surface radiance for the ambient sea surface in the infrared. In our simulator, an area of ambient sea surface detected by one pixel of the receiver is considered as an ensemble of facets. Each facet has its orientation defined by its upwind and crosswind slopes on the sea surface which is driven by the wind. Each facet acts simultaneously as source which emits its own thermal infrared radiance toward a receiver and as a mirror to reflect the sky radiance. In this report, we present an extended version of our Sea Surface Radiance Simulator (SSRS). A sky radiance model based on third party software ShipIR and atmospheric propagation software MODTRAN are incorporated to include a realistic distribution of sky radiance. A model of the turbulent wake roughness and temperature spatial variation are presented and a model of the turbulent wake radiance is implemented in our simulator.

Significance: We have integrated a model of the sea surface roughness and temperature variation in the turbulent wake into our sea surface radiance simulator to perform numerical computations of the sea surface radiance of the turbulent wake. As a result, we can compute the contrast radiance of the turbulent wake over a broad range of atmospheric, sky conditions and receiver positions. This wake contrast is important in assessing the total signature and hence vulnerability of ships.

Future work: This report is the second in a sequence of documents that describe the development and validation of our sea surface radiance simulator. Subsequent documents will

present the integration of a model of the Kelvin wake component to our simulator, the white water wake and the validation of the simulator results and performance with measured data from different observer angles, different sun elevations, different contrasts between the sea surface temperature and air temperature, different ship speeds, different hull geometries and different propeller specifications.

Sommaire

Sea Surface Infrared Radiance Simulator: Part 2: Sky radiance and trailing wake integration

Vivian Issa, Zahir A. Daya ; DRDC Atlantic TM 2011-325 ; Recherche et développement pour la défense Canada – Atlantique ; août 2012.

Contexte : Le système de propulsion des navires crée des traces, appelés sillages, qui peuvent être observés jusqu'à plusieurs kilomètres et qui persistent plusieurs minutes après le passage du navire. Ces sillages sont composés de trois parties : le sillage de Kelvin, le sillage turbulent et le sillage d'écume. Le sillage turbulent est un sujet d'intérêt pour différents types d'imagerie telle que l'imagerie optique, radar, microonde ainsi que l'imagerie infrarouge. Dans l'infrarouge, ces sillages sont encore plus riche en information puisque la surface de l'eau agit à la fois comme une propre source d'émission et comme un miroir qui réfléchit la radiance incidente. Comme la température de l'eau dépend de sa profondeur, le mixage de l'eau causé par le système de propulsion crée un sillage turbulent qui a une température différente de l'eau ambiante et ainsi une radiance infrarouge différente.

Résultats principaux : Lors d'une publication antérieure, nous avons développé une approche pour modéliser et simuler la radiance infrarouge de la surface de l'eau. Dans notre simulateur, chaque zone géographique détectée par un pixel du récepteur est considérée comme un ensemble des facettes. Les différentes facettes se distinguent par les valeurs de leurs pentes selon la direction parallèle et perpenduculaire à la vitesse du vent. Chaque facette agit à la fois comme un miroir qui réfléchit la radiance incidente et comme une propre source infrarouge. Ce document présente deux modules ajoutés à notre simulateur de la radiance infrarouge de la surface de l'eau. Un modèle de la radiance du ciel basé sur le logiciel ShipIR qui utilise le logiciel MODRAN de la propagation atmosphérique a été incorporé dans notre simulateur afin d'inclure une distribution réaliste de la radiance du ciel. De plus, nous avons implémenté un modèle du sillage turbulent avec une dépendance spatiale de la rugosité et de la température de la surface de l'eau.

Importance : Nous avons rajouté, à notre simulateur de la surface de l'eau, des modules avec une dépendance spatiale de la rugosité et de la température qui permettent de simuler la radiance infrarouge du sillage turbulent pour un ciel non uniforme. Le système simule le contraste entre la radiance infrarouge du sillage turbulent et celle de la surface de l'eau ambiante, pour des conditions atmosphériques et des positions de détecteur variables. Ce contraste est d'une grande importance pour l'étude de la signature infrarouge des navires et donc de leur vulnérabilité.

Recherches futures : Ce document est le deuxième d'une série de documents qui décrivent le développement et la validation de notre simulateur infrarouge de la radiance de la surface de l'eau. Des documents ultérieurs suivront pour présenter l'intégration, au simulateur, du sillage de Kelvin et celui d'écume, ainsi que sa validation à l'aide des données expérimentales mesurées à partir de différentes positions du récepteur, conditions atmosphériques et différents vitesses, formes de coque et systèmes de propulsion des navires.

Table of contents

List of figures

List of tables

This page intentionally left blank.

1 Introduction

Everyone has already noticed these long scars, called trailing wakes, behind boats, ships or any propelling bodies on the sea surface. Observed in detail, the trailing wake is composed of three features: the Kelvin wake, the turbulent wake, and the white water wake. The Kelvin wake is the $'V'$ shape structure with a well defined fixed angle of $35°28'$ boundary lines that can be observed in the flow direction opposite to any moving object on the sea surface or any fixed object in a stream of flowing water. The Kelvin wake is a well studied phenomenon [1–4]. The white water wake and its foamy water are complex dynamic structures with random dispersions of air bubbles in the sea water near the sea surface. They are generated at the bow and at the propeller. The turbulent wake is the smooth slightly divergent area that can persist on the sea surface for an hour or more and can be observed up to 100 km behind the ship [5]. The turbulent wake has been observed in several types of surveillance such as optical, SAR, Radar, Microwave as well as in the infrared [5–10].

In the infrared, the above features are equally well observed as in the other types of imagery. The variation in the sea surface elevation of the Kelvin wake highly affects the orientation of the sea surface facets and consequently its infrared radiance. The white water wake is a strongly scattering medium which is created by the bow and propeller. The turbulent wake is usually cooler and smoother than the background. As the sea temperature often varies significantly with depth, the turbulent wake created by the mixing effect of the propulsion system has a different temperature than the ambient sea surface.

In a previous paper [11], we developed an approach to modeling and simulating the sea surface radiance for the ambient sea surface in the infrared. In our simulator, the area from the ambient sea surface detected by one pixel of the receiver is considered as an ensemble of facets. Each facet has its orientation defined by its upwind slopes z_x and crosswind slopes z_y while the sea surface is driven by a wind with speed w m/s. Each facet acts simultaneously as source which emit its own thermal infrared radiance $L_e(\theta_r, \phi_r)$ toward a receiver located at $R(\theta_r, \phi_r, h_r)$ and as a mirror to reflect the sky radiance $L_r(\theta_r, \phi_r)$. Hence, the total radiance outgoing from a facet contains two contributions: the emitted part is approximated by the law of blackbody radiation $P(T, \lambda)$ and the reflected part is the geometric reflection of sky radiance. Further details about this approach are given in references [8, 11–13].

In this report, we present an extended version of our Sea Surface Radiance Simulator (SSRS). A sky radiance model based on third party software ShipIR and atmospheric propagation software MODTRAN are incorporated to include a physically accurate distribution of sky radiance. A model of the turbulent wake roughness and temperature spatial variation are presented and a model of the turbulent wake radiance is implemented in our simulator. In section 2 we present briefly the top level algorithm of the sea surface radiance simulator and the integration of the non-uniform sky radiance. In section 3 we present the turbulent wake radiance model. Results and discussion of the effect of the roughness and temper-

ature on the radiance of the turbulent wake are presented respectively in subsections 3.1 and 3.2 where we have also analyzed the effect of the receiver orientation on the received radiance from the turbulent wake.

2 Framework of the Sea Surface Infrared Radiance Simulator and integration of a non-uniform sky radiance

We used ShipIR to generate sky radiance $L_s(\theta_s, \phi_s)$ data using MODTRAN4. In Table 1 we list the different parameters of the atmosphere simulated with ShipIR for the example studied in this paper. Geographical and temporal information such as position and time, as well as climatic information such as wind speed and direction, sea and air temperatures, were specified in ShipIR in order to generate the sky radiance data. The output data, generated by ShipIR and exported to csv files, contains the spectral thermal emission of the atmosphere L_{atm}, the spectral indirect solar radiance L_{scat} and the spectral direct sun radiance L_{sun}. L_{atm} is a function of the air temperature and the zenith direction. L_{scat} is scattered mostly by water molecules and dust particles in the atmosphere. L_{scat} is highly dependent on the air mass parameter, the relative humidity, the zenith angle, and the azimuth angle. L_{sun} is the direct sun radiance, so it is dependent on the solar zenith and azimuth angles. Figure 1 shows the algorithm of SSRS that takes into account daylight sky radiance and non uniform sea surface roughness.

Table 1: *Example of entries to ShipIR to generate the sky radiance*

Sky Type	Clear without clouds
Wind Direction	North (90°)
RH	76%
Ambient Temperature	15.3°C
Location	Long 63.1 Lat 44.2 Az 207.729
Time	2000 GTM
Sun position	Az 204.73 Zen 74.85

At night time, the sky radiance is only dependent on the zenith angle because L_{atm} is the most significant component when we don't take into account the lunar and star radiances. Figure 2 shows an example of the dependence of the sky radiance on the zenith angle generated by ShipIR for a clear night sky and low wind scenario. We developed a program to convert the ShipIR output csv files into .mat files that can be read by MATLAB. The data is compiled to generate a matrix of the total sky radiance as a function of the zenith angle and the wavelength.

In day time, the sky radiance is zenith and azimuth dependent. We developed a program to convert the ShipIR output csv files into .mat files that can be read by MATLAB. In this case, the data is compiled to generate, for each wavelength, a matrix of the total sky radiance as a function of the zenith and azimuth angles. Each matrix contains the total sky radiance of the three components L_{atm}, L_{scat} and L_{sun}. In Figure 3 we show the data structure and the conversion process. This program can be used to generate the sky radiance for night time. However, to reduce the computing time, the night time case was treated with a different code as it is only zenith dependent.

We show in Figure 1 the top level algorithm of the sea surface radiance simulator. The function *DayCSVtoMatlab.m* converts the sky radiance data from csv files into *.mat* file for each wavelength. Each *.mat* file contains the total spectral sky radiance matrix dependent on the zenith and azimuth angles. In night time case, the output of *NightCSVtoMatlab.m* will be a *.mat* file that contains a matrix dependent on the zenith angle and the wavelength.

The geographical space of the sea surface is divided into four parts: background zone, turbulent wake zone, Kelvin wake zone and foamy white water wake zone. The background zone was addressed in a previous document [11] and the turbulent wake is treated in this paper. The main difference amongst the first three zones is the roughness function that describes the variance of the probability density function of facet slopes. In the background zone, this variance is constant while it varies in the turbulent wake and in the Kelvin wake. The roughness function of the turbulent wake is described in section 3. Each zone is discretized and the *Roughness.m* function is used to generate its roughness distribution function.

For each point of the discretized space, the relative receiver position, the map of the different possible facets, and their probability density function are generated using the functions *ReceiverRelPosition.m* and *CoxAndMunk.m*. The function *Geo.m* generates the geometrical parameters for each possible facet such as the sky orientation seen by each facet, the normal orientation to the facet, and all the parameters necessary to find the probability density function for the slopes as described in an earlier paper [11]. The part of the sky to be reflected on each possible facet as well as the optical properties, the spectral sea surface intrinsic radiance, and the spectral sky radiance reflected on the sea surface are computed. Finally, the total radiance of the discretized space is computed for the whole wavelength band.

3 Turbulent wake radiance: results and discussion

As described in an earlier paper [11], the sea surface radiance has two main sources: the intrinsic thermal radiance emitted from the sea, and the sky radiance reflected off the sea

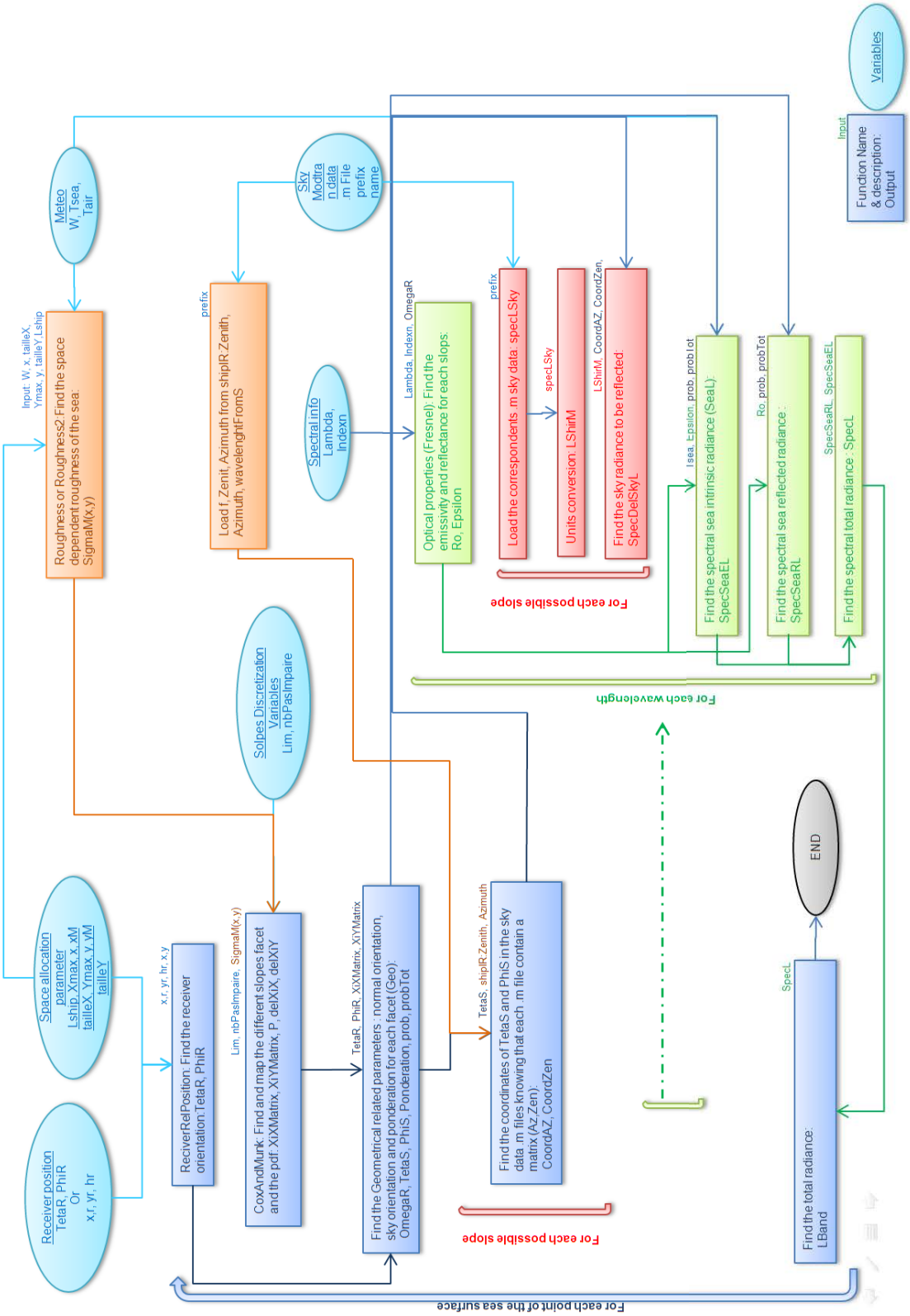

Figure 1: *Top Level algorithm of the Sea Surface Radiance Simulator.*

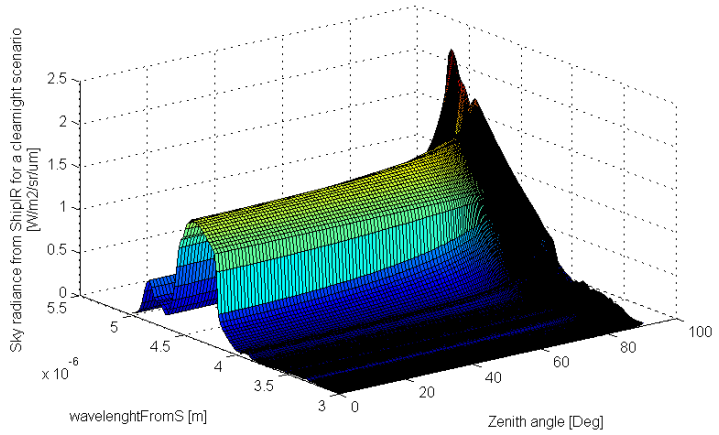

Figure 2: *Sky radiance from ShipIR for a clear night sky and low wind conditions.*

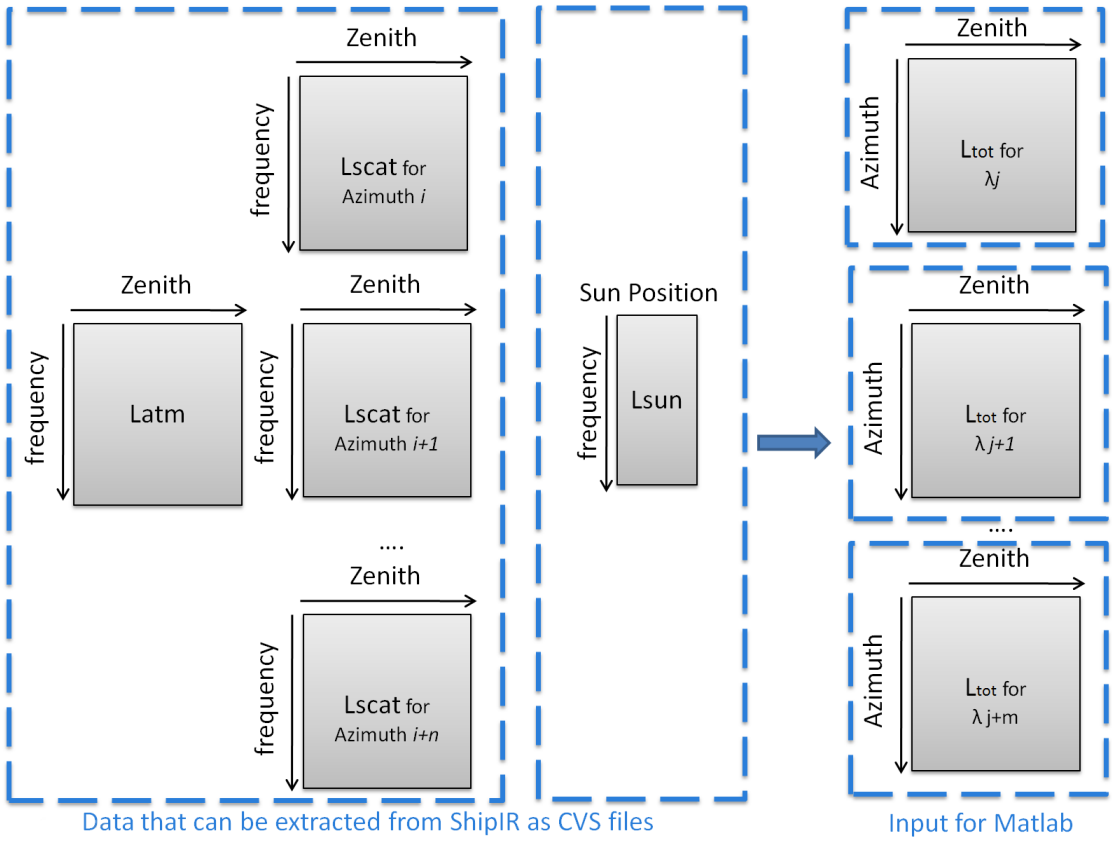

Figure 3: *Data handling in the SSRS.*

surface. Furthermore, the reflectivity and emissivity varies with ω_r, the angle between the receiver and the normal to the surface. When ω_r increases, the reflectivity increases as well and vice versa (Figure 5). When the roughness is low, facets with low slopes have the highest probability of occurrence. This means that the value of ω_r is close to the value of the receiver zenith angle θ_r. Therefore, low zenith angles of the receiver will preferentially receive emitted radiance while high θ_r will mainly receive reflected radiance. Figure 4 shows the co-ordinate system and the geometry of a sea surface facet.

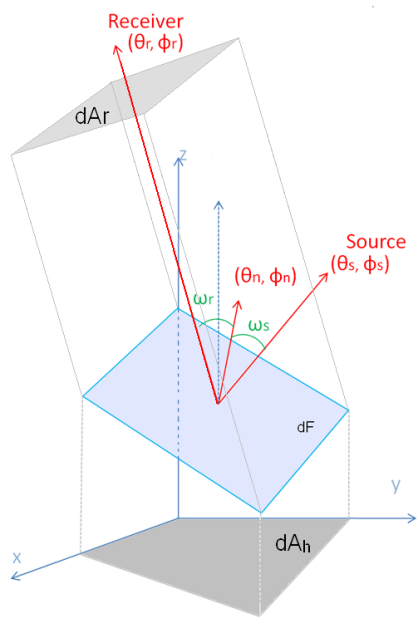

Figure 4: *The co-ordinate system and the geometry of a sea surface facet.*

The turbulent wake can be distinguished from the sea surface background by its different roughness and temperature. The turbulent wake is generally cooler and smoother than the ambient ocean. The sea temperature directly affects the emitted part of the sea radiance. The roughness affects both emitted and reflected radiances by its effect on ω_r. In the next two subsections we describe a model of a trailing wake with the effect of the roughness variation on the sea surface radiance and the combined effect of the temperature and the roughness on the total radiance.

3.1 Model of the turbulent wake on the sea surface roughness

The turbulent wake is the relatively smooth centerline wake starting just after bubbly turbulent zone behind the ship. This zone is relatively smooth because of the attenuation of the short waves by the ship generated turbulence, upwelling attenuation by viscosity and

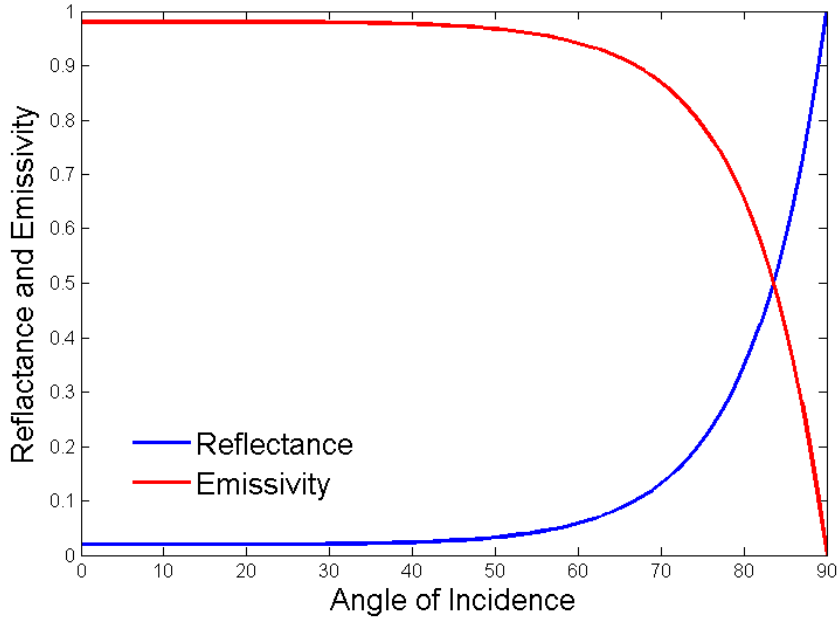

Figure 5: *The dependence of emissivity and reflectivity of the sea surface on the angle of incidence.*

surface tension. As all these damp short waves, we assume that in the trailing wake the roughness of the surface is inversely proportional to the turbulence intensity. The turbulence intensity of the trailing wake varies with distance downstream from the ship and is given by [10, 14–17]:

$$U_{rmsx} \propto x^{-\frac{4}{5}}, \tag{1}$$

where x is the downstream distance. The dependence of the turbulence intensity in the cross-stream direction (y) is given by is given by

$$U_{rmsy} \propto \left(1 - \frac{1}{2}\xi^2\right) e^{-\frac{1}{2}\xi^2} \tag{2}$$

where

$$\xi = \frac{y}{l(x)} \tag{3}$$

and

$$l \propto x^{\frac{1}{5}}. \tag{4}$$

Hence, we build a roughness function for the turbulent wake with a cross-stream and downstream variation which is inversely proportional to the turbulence intensity and approaches the background roughness from the ship. We also constrained this function to be valid for $|y|\,l$, the cross-stream width of the turbulence intensity function. The resulting far away roughness function is given by:

$$\sigma_{TW}^2 = \left[\frac{1}{U_A * U_{rmy} * U_{urmx} + U_B}\right] * \alpha + (1-\alpha) * \frac{1}{U_B}. \tag{5}$$

where U_A is the maximum turbulence intensity that corresponds to the minimum roughness, and U_B is the turbulence intensity of the background with

$$\alpha = \begin{cases} 0 & \text{if } y > l \\ 1 & \text{if } y \leq l \end{cases}. \tag{6}$$

For an isotropic Cox and Munk probability distribution case [11], the roughness is represented by the variance of the probability density function of slopes and is given by:

$$\sigma_{CM}^2 = \frac{0.003 + 0.00512W}{2}, \tag{7}$$

where W is the wind speed. From equation 7 we can see that for a smooth sea ($wind = 0$ m/s) the variance is $\sigma_A^2 = 0.0015$. This allows us to determine the constants $U_A = \frac{1}{\sigma_A^2}$ and $U_B = \frac{1}{\sigma_{CM}^2}$.

In Figure 6 we have plotted an example of turbulence intensity and roughness in the trailing wake for a 2 m/s wind speed. In Figures 7 and 8 we illustrate the roughness and turbulence intensity of the central line of the turbulent wake for the same example. We can see in the logarithmic plots these two figures that the downstream turbulence intensity is $U_{rms} = U_A * x^{-4/5} + U_B$.

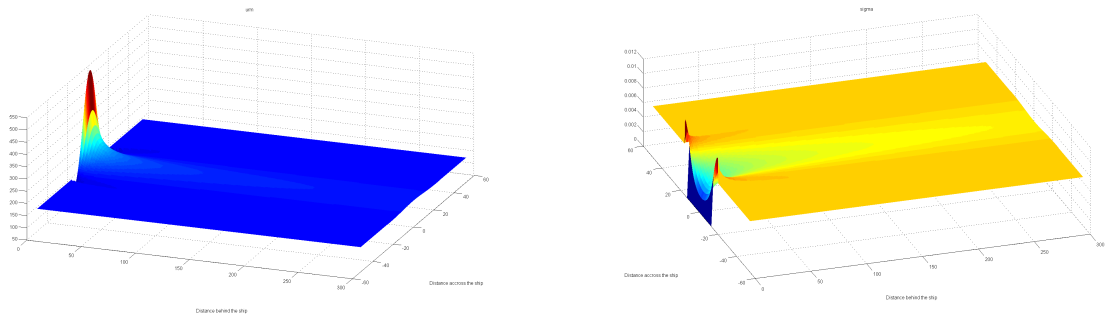

Figure 6: *Turbulence intensity (left) and sea surface roughness (right) of the trailing wake*

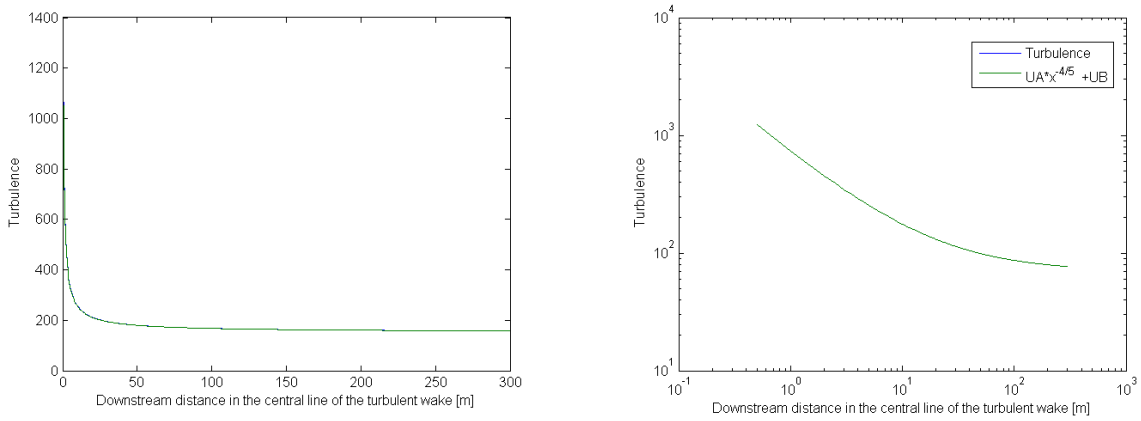

Figure 7: *The turbulence intensity along the central line of the turbulent wake (linear scale - left, logarithmic scale - right)*

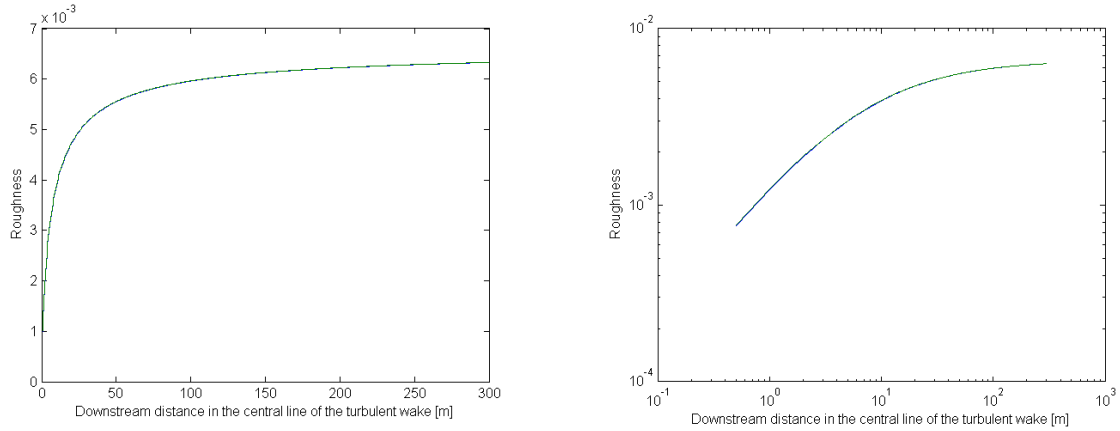

Figure 8: *The roughness of the central line of the turbulent wake (linear scale - left, logarithmic scale - right)*

In Table 2 we have listed the different cases simulated to generate both the radiance of the central line of the turbulent wake given by the function described previously and the radiance of the background at the same geographical location (without roughness variation). In order to observe the effect of the roughness independent of the temperature dependence on the radiance of the turbulent wake, the temperature of the turbulent wake is considered uniform and equal to the temperature of the background in all the cases treated in this subsection.

The sky radiance used for these simulations was generated for the day time in Table 1.

In Figure 9 and 10 we have plotted for the various cases simulated, the radiance calculated along the central line of the trailing wake for the background and turbulent wake. In addition we have plotted the contrast between the turbulent wake radiance (L_{TW}) and the background radiance (L_{bck}) as described below:

$$contrast = \frac{L_{TW} - L_{bck}}{L_{bck}} \tag{8}$$

Overall, these results demonstrate that the radiance of the trailing wake is strongly dependent on the receiver position.

Table 2: *Different cases for the central line of the trailing wake*

Case	Wind Speed [m/s]	Receiver [m]	Sea Temperature [C]
1	5	0,0,500	12
2	5	0,0,500	8
3	5	0,0,500	4
4	5	0,0,50	4
5	5	150,-150,150	4
6	4	0,-1150,100	4

Figure 9 shows the radiance of the central line of the turbulent wake for cases 1 to 3. Even though decreasing the temperature of the sea surface decreases the thermally emitted sea surface radiance and hence the total radiance, the absolute value of the contrast between the background and the trailing wake for these cases is smaller than 0.05%. It is important to note that the receiver in these cases is located at (0,0,500). For this receiver position, θ_r throughout the turbulent wake varies from 0°to 40°. As the roughness is low in the turbulent wake, ω_r is close to θ_r resulting in a small reflectivity coefficient for these values of θ_r. Consequently the roughness variation in the trailing wake does not significantly affect the total radiance of the turbulent wake. In fact, for small receiver angles, the contribution of the reflected sky radiance is smaller than the thermal emitted radiance and no effect of the roughness variation can be observed.

In case 4, the observer is located at (0,0,50) and the receiver relative zenith angle θ_r varies from 0°to 80.5°. A contrast up to 1.75% between the turbulent wake and the background is observed in the Figure 10. For further distance downstream, where θ_r is larger, the effect of roughness on the radiance of the trailing wake observed via the contrast is much higher than for smaller θ_r. To further highlight the effect of high θ_r, case 5 considers a small θ_r and case 6 consider high θ_r. Case 6 with θ_r of about 85° shows a high contrast between the turbulent wake and the background. This confirms that the roughness variation in the turbulent wake affects the total radiance of the turbulent wake for high receiver angles.

3.2 Model of the turbulent wake on the sea surface temperature

The temperature of sea water varies with depth. In ship wakes, the propeller brings up colder water into the sea surface of the trailing wake. Hence the turbulent wake has a different temperature from the background sea surface. The wake temperature slowly relaxes in time so that it tends to the background sea surface temperature. Assuming that the temperature variation follows the downstream and cross-stream roughness dependencies, we propose a function to simulate a temperature variation in the trailing wake:

$$T = [T_y - T_{bck}]\, x^{-\frac{4}{5}} + T_{bck}\,, \tag{9}$$

where T_{bck} is the ambient sea surface temperature, and

$$T_y = \frac{1}{\left[(U_{rmsy} - U_0) * A + \frac{1}{T_{bck}}\right]\alpha + (1-\alpha)\frac{1}{T_{bck}}}\,. \tag{10}$$

In the above, U_{rmsy} and α are as defined previously, $U_0 = -e^{-2}$ the minimum of the function U_{rmsy}, $A = \frac{U_{TA} - U_{TB}}{1 - U_0}$ and $U_{TA} = \frac{1}{T_A}$ where U_{TA} is the minimum temperature in the trailing wake. As an example, we considered that the mixing due to the propeller brings down the temperature to a minimum of $T_A = T_{bck} - 4°C$ for which we have simulated the radiance of the turbulent wake as well as the radiance of the background. In Figure 11 we show for this example the temperature profile of the turbulent wake as a function of the downstream and cross-stream distances.

To compare the effect of roughness and temperature variation on the radiance of the turbulent wake, we simulate the radiance toward receivers at two different positions. The first receiver position (0,-1150,100) has a large zenith angle of 85° while the second receiver

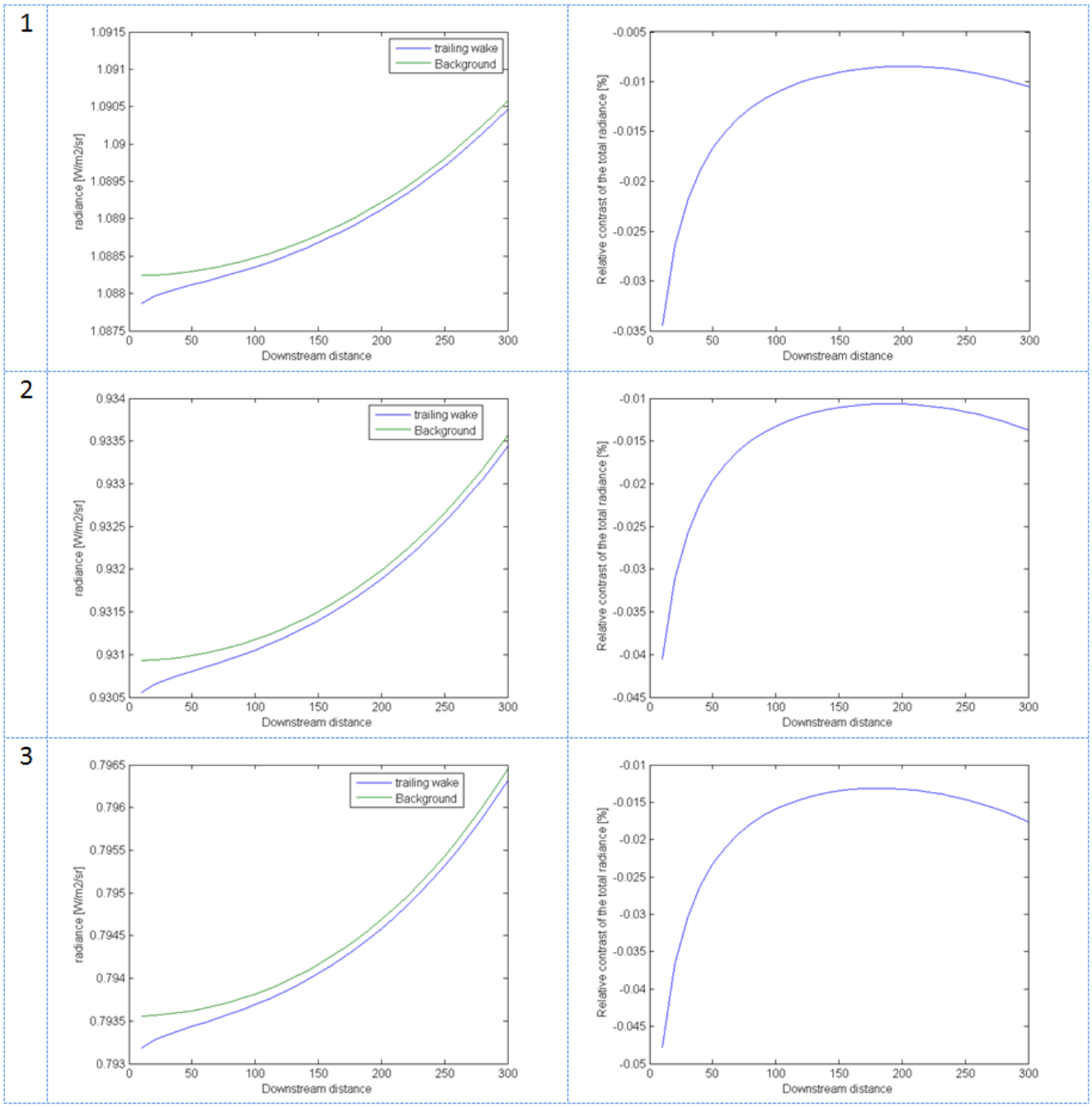

Figure 9: *For cases 1 to 3: Total radiance along the center line of the turbulent wake and the background total radiance for the same position (left). Percentage difference between the turbulent wake and the background (right).*

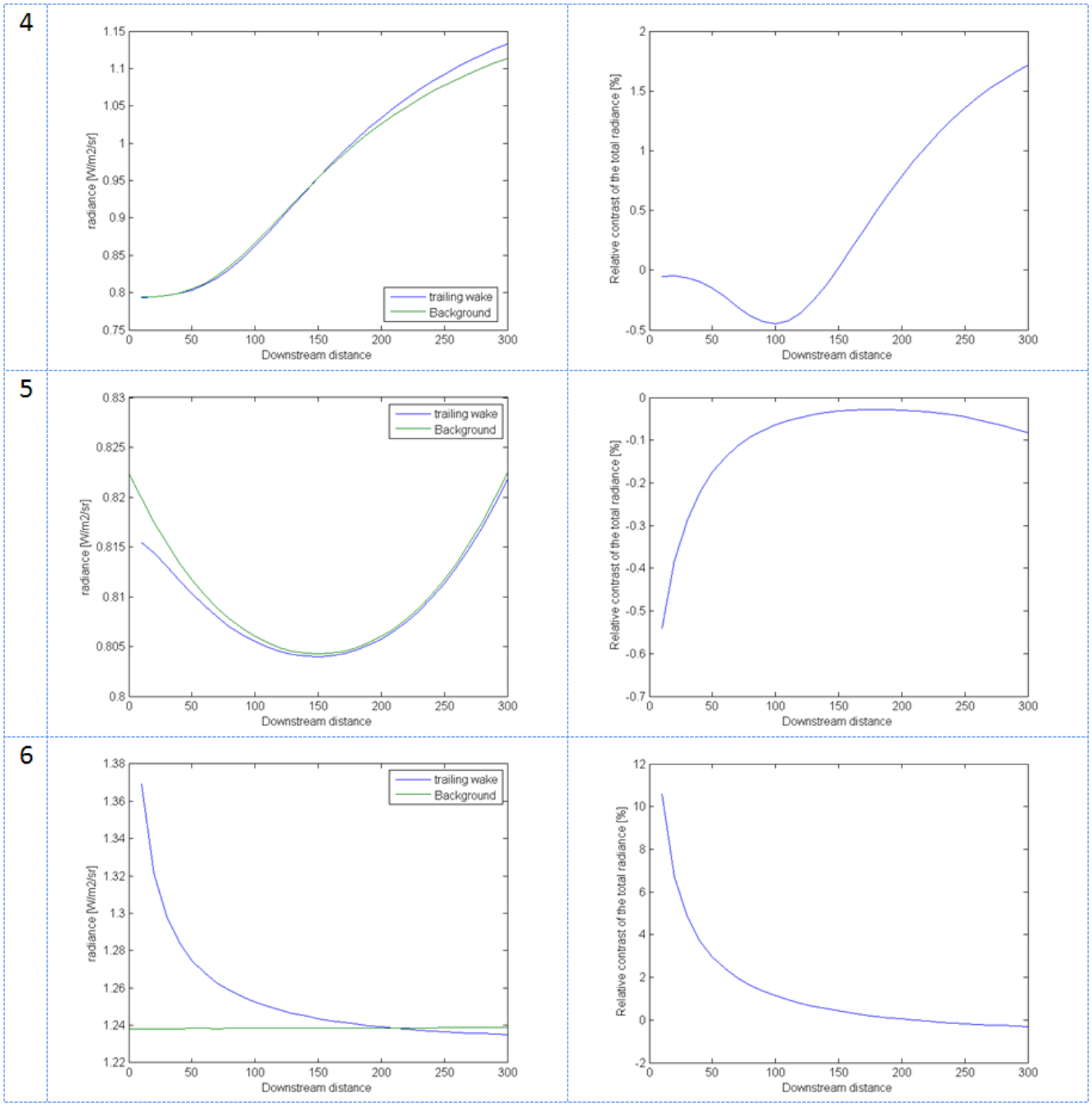

Figure 10: *For cases 4 to 6: Total radiance along the center line of the turbulent wake and the background total radiance for the same position (left). Percentage difference between the turbulent wake and the background (right).*

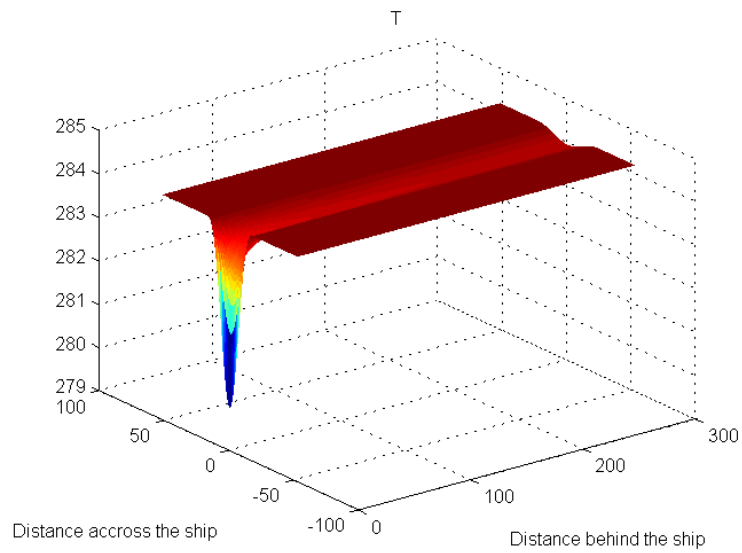

Figure 11: *Temperature of the turbulent wake as a function of the downstream and cross-stream distances for a receiver at (0,-1150,100).*

position (0,-1000,+1000) has a relatively small zenith angle of 45°. In Figures 12 and 14 we plot 4 cases (i) the sea surface radiance of the background, (ii) the radiance of the trailing wake with variable temperature, (iii) the radiance of the trailing wake with variable roughness and (iv) the radiance of the trailing wake with a variable temperature and roughness toward these receivers. From the first receiver, the turbulent wake can be seen brighter than the background while from the second receiver, it can be seen darker. We explain in the next two subsections the reasons for these positive and negative contrasts.

3.2.1 An example of positive contrast between the turbulent wake and the background

A high receiver zenith angle implies a large sea surface reflectivity coefficient and small emissivity coefficient when the sea surface is flat (Figure 5). When the roughness increases, the probability of occurrence of sea surface facets with high slopes increases as well. In fact, for a receiver with a high zenith angle, the angle ω_R between the receiver and the normal to those facets is more likely to decrease compared to a horizontal facet (Figure 13). Hence the emissivity coefficient increases and consequently the thermal emitted radiance grows. As well the reflectivity coefficient decreases and thus the sky reflected radiance diminishes. At the same time, the zenith angle parts of the sky reflected on those facets is smaller than the zenith angle parts of the sky reflected on a flat sea surface, which further decreases the reflected sky radiance as the sky radiance generally increases with its zenith angle. As a result of the roughness variation in the trailing wake, the total radiance of the trailing wake decreases when the roughness increases in the downstream direction. We

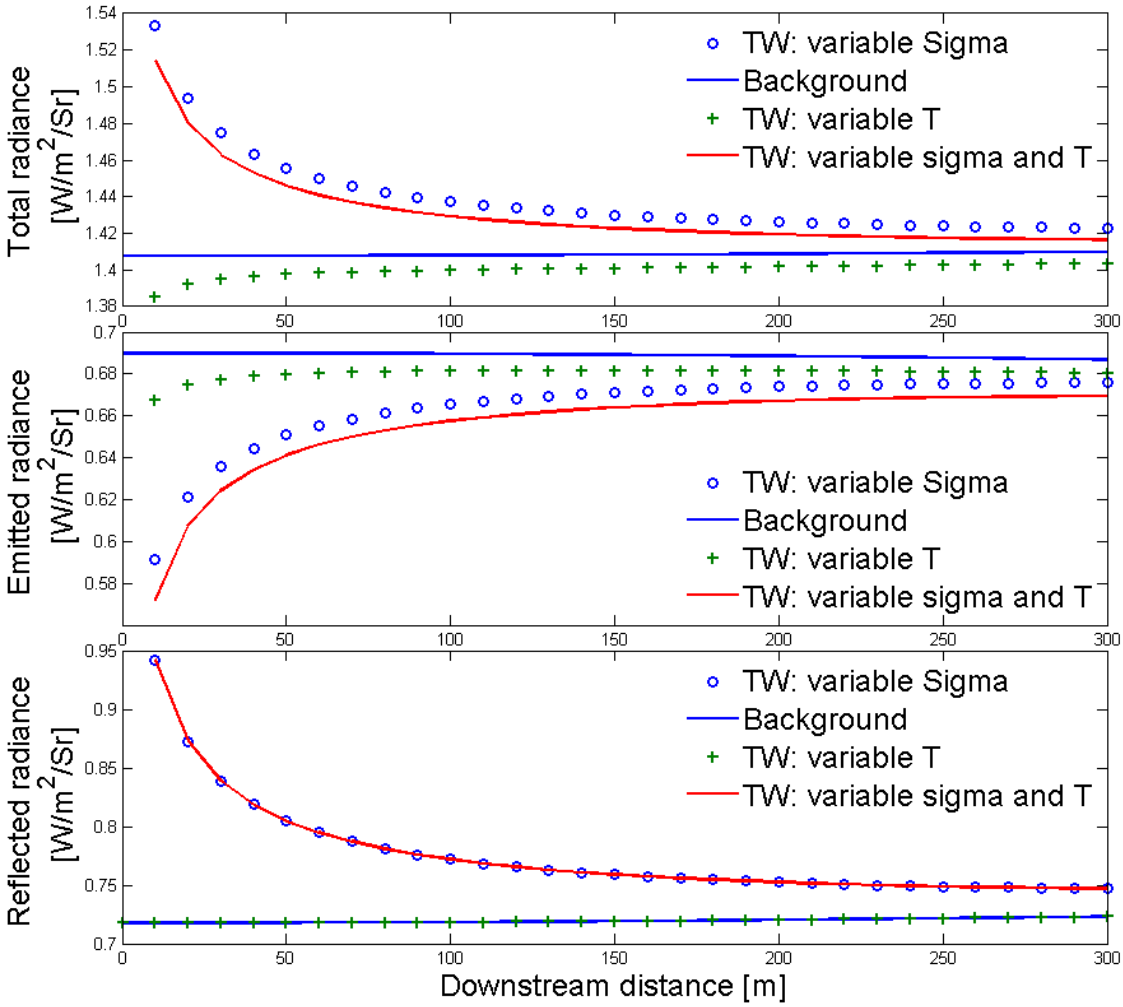

Figure 12: *The total radiance (top), the emitted radiance (middle) and the reflected radiance (bottom) of the background (blue line), the trailing wake with a variable roughness and constant temperature (the circle symbol), the trailing wake with variable temperature and constant roughness (the plus symbol), the trailing wake with variable temperature and roughness (red line) toward receiver at (0,-1150,100).*

show this roughness variation effect on the total, emitted and reflected radiance in Figure 12 with the circle symbol.

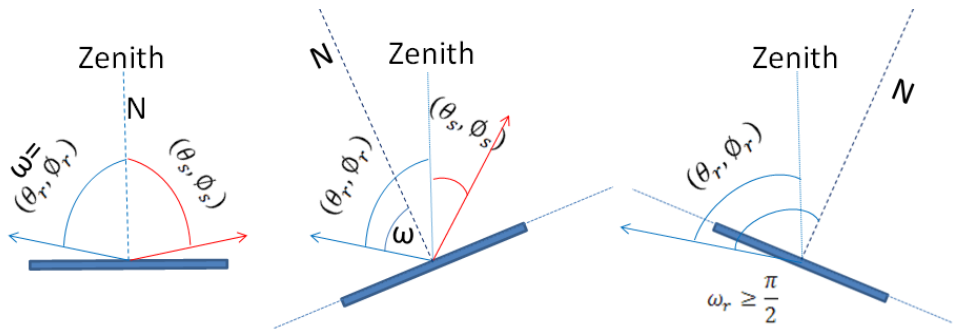

Figure 13: *Examples of the the geometry for a receiver at a high zenith angle (left) with no roughness (middle) example of a high roughness: ω increases but θ_s decreases (right) example of a high roughness: hidden facet*

With increasing temperature, the emitted radiance of the sea surface increases as well but reflected part is not affected. Hence the total radiance of the trailing wake increases in the downstream direction. We show this temperature variation effect on the total, emitted and reflected radiance in Figure 12 with the plus symbol.

For a high receiver angle the reflectivity coefficient is high and emissivity coefficient is low, hence the variation in the reflected radiance can overcome the variation in the emitted radiance. Figure 12 shows the roughness and temperature variation effect with the red line, and we can see that the roughness variation overcomes the temperature variation. The increase in the total radiance of the trailing wakes compared to the background gives a positive contrast which decreases downstream until it reaches the radiance of the background.

3.2.2 An example of negative contrast between the turbulent wake and the background

In the case of a low zenith receiver angle, the sea surface reflectivity coefficient is small and its emissivity coefficient is large when the sea surface is flat (Figure 5). Unlike the case of a high receiver angle, here when the roughness increases for a low receiver angle, the angle ω_R between the receiver and the normal to those facets increases compared to a flat facet, hence the emissivity coefficient decreases and the reflectivity coefficient increases. Consequently, the thermal emitted radiance decreases and the sky reflected radiance increases. At the same time, the zenith angle of the parts of the sky reflected on those facets is more likely to increase compared to the zenith angle of the sky parts reflected on a flat sea surface. This further increases the reflected sky radiance so the sky radiance increases with its zenith angle (Figure 15). As a result of the roughness variation in the trailing wake, the total radiance of the trailing wake will increases with roughness. We show this roughness

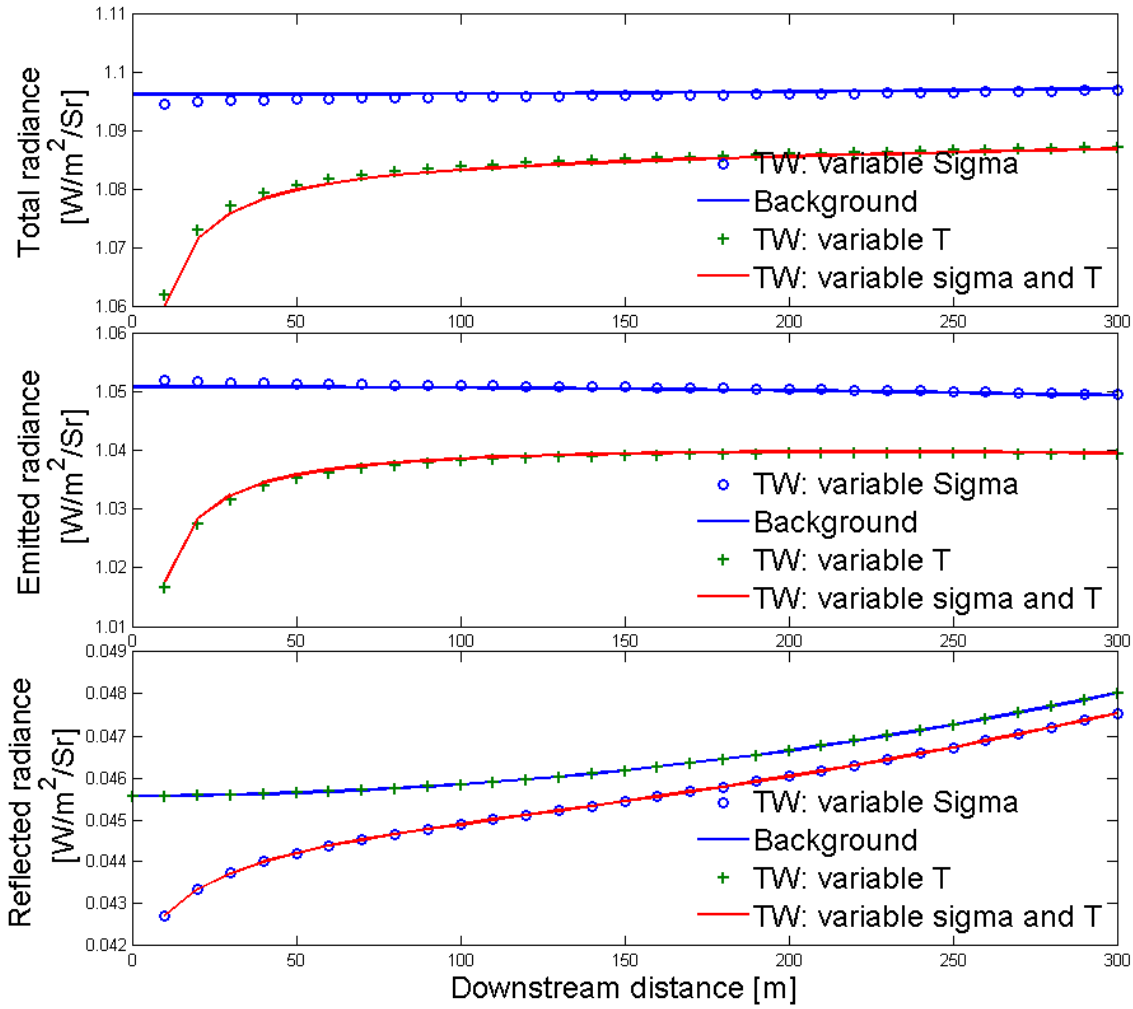

Figure 14: *The total radiance (top), the emitted radiance (middle) and the reflected radiance (bottom) of the background (blue line), the trailing wake with a variable roughness and constant temperature (the circle symbol), the trailing wake with a variable temperature and constant roughness (the plus symbol), the trailing wake with a variable temperature and roughness (red line) toward a receiver at (0 -1000 1000)*

variation effect on the total, emitted and reflected radiances in Figure 14 with the circle symbol.

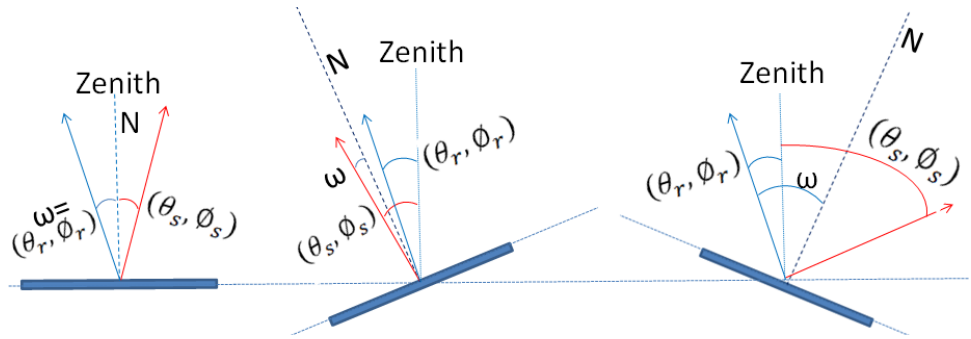

Figure 15: *Examples of the the geometry for a receiver at a low zenith angle (Left) with no roughness (middle) example of a high roughness:* ω *decreases but* θ_s *increases (right) example of a high roughness:* ω *and* θ_s *increase*

Similar to the previous example, the emitted radiance increases with the temperature while the reflected part is not affected. Hence the total radiance of the trailing wake increases in the downstream direction. We show this temperature variation effect on the total, emitted and reflected radiances in Figure 14 with the plus symbol.

As the emissivity coefficient is high for a low zenith receiver angle, a variation in the emitted radiance can dominate the variation in the reflected radiance which explains the negative contrast in the trailing wake of this example. The red line in Figure 12 shows the roughness and temperature variation effect with distance.

4 Conclusion and Future Work

In this report, the integration of a non uniform sky radiance and the trailing wake model are presented in updating our sea surface radiance simulator. We used ShipIR to generate sky radiance data using MODTRAN4. We also added a model of the roughness and temperature variation in the turbulent wake and a numerical computation of the radiance of the turbulent wake.

We found that the receiver position highly affects the simulated contrast between the radiance of the trailing wakes and that of the background. In the turbulent wake, decreasing the receiver zenith angle decreases the contribution of the sky radiance by decreasing the reflectivity of the sea surface while increasing of the receiver zenith angle will decreases the thermal emitted sea surface radiance by decreasing its emissivity. Furthermore, the effect of the roughness variation of the turbulent wake can be more strongly observed from high receiver zenith angle and the effect of temperature variation of the turbulent wake can be more strongly observed at low receiver zenith angle.

In a subsequent paper the model of the Kelvin wake component will be integrated into our simulator. Sea surface elevation in the Kelvin wake will be calculated and from this elevation, the orientation of the different facets on the sea surface will be deduced. Hence, the radiance of the Kelvin wake area can be predicted. In the future we plan to validate the simulator results with measurement data. If needed, an update of the model with consideration of the multiple reflection and shadowing will be developed. A sea trial should be conducted to collect measured data from different observer angles for different sun elevations and different contrasts between the sea surface and air temperatures. The trial should vary the ship speed so as to validate the radiance of the Kelvin wake predicted by our simulator. Thereafter, we plan to model the radiance of the white water wake in the infrared.

References

[1] Reed, A. M. and Milgram, J. H. (2002), Ship wakes and their radar images, *Annual Review of Fluid Mechanics*, 34, 469–502.

[2] Hally, D. (1997), Wave amplitude in the far wake of CF ships, DREA TM 1997-220, Defence Research Establishment Atlantic.

[3] Hally, D. (1993), Dispersion analysis of an unsteady free surface panel method, DREA TM 1993-211, Defence Research Establishment Atlantic.

[4] Zilman, G., Zapolski, A., and Marom, M. (2004), The speed and beam of a ship from its wake's SAR images, *IEEE Transactions on Geoscience and Remote Sensing*, 42(10), 2335–43.

[5] Peltzer, R., Garrett, W., and Smith, P. (1985), A remote sensing study of a surface ship wake, *Ocean Engineering and the Environment*, 86, 277.

[6] Garrett and Smith (1984), Physical and Chemical Factors Affecting the Thermal IR Imagery of Ship Wakes, NRL Memorandum, Report 5376, Naval Research Laboratory.

[7] Stewart, M. (1988), Numerical Prediction of Thermal Ship Wakes, *OED (ASME, Ocean Engineering Division)*, 13, 145–153.

[8] Schwartz, I. B. and Priest, R. G. (1988), Reflection driven ship wake contrasts in the infrared, NRL Memorandum, Report 9144, Naval Research Laboratory.

[9] Chen, J., Chen, B., and Yang, J. (2009), The turbulent wake detection and beam estimation of a ship in SAR images, *International Workshop on Geoscience and Remote Sensing (ETT and GRS)*, 1, 230–3.

[10] Daya, Z. A. and Galloway, C. (2010), Infrared Intensity of the trailing turbulent surface wake of CFAV Quest in trial Q300, DRDC Atlantic TM 2010-175, Defence R&D Canada - Atlantic.

[11] Issa, V. and Daya, Z. A. (2010), Sea Surface Infrared Radiance Simulator Part 1: Roughness and Temperature models of the Sea Surface Radiance, DRDC Atlantic TM 2010-280, Defence R&D Canada - Atlantic.

[12] Cox, C. and Munk., W. (1954), Measurement of the Roughness of the Sea Surface from Photographs of the sun Glitter, *Journal of the Optical Society of America*, 44, 838.

[13] Zeisse., C. R. (1995), Radiance of the Ocean Horizon, *Journal of the Optical Society of America*, 12, 2022.

[14] Daya, Z. A. (2009), Mid-wave IR contrast intensity of Quest wake from the air in Q300, NATO TG-79 Fall meeting minutes.

[15] Tennekes, H. and Lumley, J. L. (1974), A first course in turbulence, The MIT press.

[16] Birkhoff, G. and Zarantonello, E. (1957), Jets, Wakes, and cavities, Academic press.

[17] Reed, A. M. and Milgram, J. H. (2002), Ship wakes and their radar images, *Annual Review of Fluid Mechanics*, 34, 469–502.

This page intentionally left blank.

DOCUMENT CONTROL DATA

(Security markings for the title, abstract and indexing annotation must be entered when the document is Classified or Designated.)

1. ORIGINATOR (The name and address of the organization preparing the document. Organizations for whom the document was prepared, e.g. Centre sponsoring a contractor's report, or tasking agency, are entered in section 8.)

Defence Research and Development Canada – Atlantic
PO Box 1012, Dartmouth NS B2Y 3Z7, Canada

2a. SECURITY MARKING (Overall security marking of the document, including supplemental markings if applicable.)

UNCLASSIFIED

2b. CONTROLLED GOODS

(NON-CONTROLLED GOODS)
DMC A
REVIEW: GCEC APRIL 2011

3. TITLE (The complete document title as indicated on the title page. Its classification should be indicated by the appropriate abbreviation (S, C or U) in parentheses after the title.)

Sea Surface Infrared Radiance Simulator: Part 2: Sky radiance and trailing wake integration

4. AUTHORS (Last name, followed by initials – ranks, titles, etc. not to be used.)

Issa, V.; Daya, Z. A.

5. DATE OF PUBLICATION (Month and year of publication of document.)

August 2012

6a. NO. OF PAGES (Total containing information. Include Annexes, Appendices, etc.)

38

6b. NO. OF REFS (Total cited in document.)

17

7. DESCRIPTIVE NOTES (The category of the document, e.g. technical report, technical note or memorandum. If appropriate, enter the type of report, e.g. interim, progress, summary, annual or final. Give the inclusive dates when a specific reporting period is covered.)

Technical Memorandum

8. SPONSORING ACTIVITY (The name of the department project office or laboratory sponsoring the research and development – include address.)

Defence Research and Development Canada – Atlantic
PO Box 1012, Dartmouth NS B2Y 3Z7, Canada

9a. PROJECT OR GRANT NO. (If appropriate, the applicable research and development project or grant number under which the document was written. Please specify whether project or grant.)

11gf

9b. CONTRACT NO. (If appropriate, the applicable number under which the document was written.)

10a. ORIGINATOR'S DOCUMENT NUMBER (The official document number by which the document is identified by the originating activity. This number must be unique to this document.)

DRDC Atlantic TM 2011-325

10b. OTHER DOCUMENT NO(s). (Any other numbers which may be assigned this document either by the originator or by the sponsor.)

11. DOCUMENT AVAILABILITY (Any limitations on further dissemination of the document, other than those imposed by security classification.)

(X) Unlimited distribution
( ) Defence departments and defence contractors; further distribution only as approved
( ) Defence departments and Canadian defence contractors; further distribution only as approved
( ) Government departments and agencies; further distribution only as approved
( ) Defence departments; further distribution only as approved
( ) Other (please specify):

12. DOCUMENT ANNOUNCEMENT (Any limitation to the bibliographic announcement of this document. This will normally correspond to the Document Availability (11). However, where further distribution (beyond the audience specified in (11)) is possible, a wider announcement audience may be selected.)

13. ABSTRACT (A brief and factual summary of the document. It may also appear elsewhere in the body of the document itself. It is highly desirable that the abstract of classified documents be unclassified. Each paragraph of the abstract shall begin with an indication of the security classification of the information in the paragraph (unless the document itself is unclassified) represented as (S), (C), or (U). It is not necessary to include here abstracts in both official languages unless the text is bilingual.)

In a previous paper, we developed a sea surface radiance simulator (SSRS) for modeling and simulating the sea surface radiance of the ambient sea surface in the infrared. In this report, we present two additional models in our simulator. A sky radiance model based on third party software ShipIR and atmospheric propagation software MODTRAN are incorporated to include a realistic distribution of sky radiance. A model of the turbulent wake roughness and temperature spatial variation are presented and a model of the turbulent wake radiance is implemented in our simulator. Our results show that the sea surface radiance is highly affected by the receiver position. In the turbulent wake, decreasing the receiver zenith angle decreases the reflected sky radiance on the sea surface and increasing the receiver zenith angle will decrease the thermal emitted sea surface radiance. This strong dependence results in positive or negative wake contrast radiances at different receiver angles.

14. KEYWORDS, DESCRIPTORS or IDENTIFIERS (Technically meaningful terms or short phrases that characterize a document and could be helpful in cataloguing the document. They should be selected so that no security classification is required. Identifiers, such as equipment model designation, trade name, military project code name, geographic location may also be included. If possible keywords should be selected from a published thesaurus. e.g. Thesaurus of Engineering and Scientific Terms (TEST) and that thesaurus identified. If it is not possible to select indexing terms which are Unclassified, the classification of each should be indicated as with the title.)

sea surface reflectivity
sea surface emissivity
sea surface roughness
infrared sea radiance
sky radiance
trailing wake
Kelvin wake
turbulent wake

This page intentionally left blank.

Defence R&D Canada

Canada's leader in defence
and National Security
Science and Technology

R & D pour la défense Canada

Chef de file au Canada en matière
de science et de technologie pour
la défense et la sécurité nationale

DEFENCE DÉFENSE

www.drdc-rddc.gc.ca